Effect of Nanoclay and ZnO on the Physical and Chemical Properties of Wood Polymer Nanocomposite

Biplab K. Deka, Tarun K. Maji

Department of Chemical Sciences, Tezpur University, Assam 784028, India

Received 18 April 2011; accepted 20 July 2011
DOI 10.1002/app.35314
Published online 3 November 2011 in Wiley Online Library (wileyonlinelibrary.com).

ABSTRACT: Wood polymer composite (WPC) was prepared by using solution blended high density polyethylene, low density polyethylene, polypropylene, and poly(vinyl chloride) with *Phragmites karka* wood flour and polyethylene-*co*-glycidyl methacrylate (PE-*co*-GMA). The effect of addition of nanoclay and ZnO on the properties of the composite was examined. The distribution of silicate layers and ZnO nanopowder was studied by X-ray diffractrometry and transmission electron microscopy. The improvement in miscibility among polymers due to addition of PE-*co*-GMA as compatibilizer was studied by scanning electron microscopy. WPC treated with 3 phr each of clay and ZnO showed an improvement in thermal stability and UV resistance. Mechanical and flame retarding properties were also enhanced after the incorporation of clay/ZnO nanopowder. Both water and water vapor absorption were found to decrease due to inclusion of nanoclay and ZnO in WPC. © 2011 Wiley Periodicals, Inc. J Appl Polym Sci 124: 2919–2929, 2012

Key words: nanocomposites; wood; organoclay; mechanical properties; thermal properties

INTRODUCTION

The northeastern part of India is rich in forest based cellulosic resources to a lucrative amount. Only a few of the different species available in this region have been explored. Nal, a type of non conventional plant available in this region, do not have any structural application.

The pollution caused by post consumer plastic materials comprising mostly of polyethylene, polypropylene (PP), polyvinyl chloride, etc. has become a matter of concern. Recycling is one of the processes to minimize the waste pollution. The poor mechanical, thermal, and other properties of recycled waste plastic materials restrict their use in a number of applications. The nonconventional plant material can be made value added material suitable for preparation of structural components by treating with waste plastic materials. Structural components include window, window profiles, table tops, partition walls, etc.

Solution blending is one of the process to mix varieties of waste plastics. No single solvent can alone be able to solubilize different kind of plastics. Moreover, it is difficult to segregate different kind of plastics. The optimization of solvent ratio can be determined properly if a mixture of known percentage of virgin high density polyethylene (HDPE), low density polyethylene (LDPE), PP, poly(vinyl chloride) (PVC), etc. is used as starting waste plastic materials.

Plant fiber reinforced polymer composite is a widespread used branch of composite materials.[1] Wood is ecofriendly, biodegradable, and renewable, but they have poor mechanical properties and dimensional stability. These properties can be improved by making composites with polymer matrix.[2,3] The main disadvantage of using wood flour (WF) to the polymer matrix is its poor compatibility to the polymer. As WFs are hydrophilic and polymers are hydrophobic in nature, there always remain an interfacial phase separation between the wood and the polymers. These results in poor compatibility among the constituents, and hence, decrease the properties of the composites. To improve the miscibility between polymers and WF, compatibilizers are used. They act as a bridging agent between the two interfaces. Compatibilizers like glycidyl methacrylate and maleated PP have significantly improved the properties of the wood polymer composite (WPC).[4,5]

Thermal stability is one of the important properties of WPC. It has been established that thermostability along with the other properties of the composite can be improved by using clay particles.[6] Research on nanometer-sized materials has increased remarkably during the past few years due to their unique characteristics of large fraction of surface atoms and a higher surface area. The addition of

Correspondence to: T. K. Maji (tkm@tezu.ernet.in).

nanoclay to the composite enhances the mechanical, thermal, and other properties. Besides using clay, different metal oxide nano particles (Si, Zn, Ti, etc.) are used to improve the properties like mechanical, thermal, flammability, weathering, etc. of the composites. The surface characteristics of nanopowders play a key role in their fundamental properties from phase transformation to reactivity. A dramatic increase in the interfacial area between fillers and polymer can significantly improve the properties of the polymer.[7] These nanoparticles are non toxic, stable, and highly themostable inorganic filler. Owing to all these properties, these are widely used in all types of materials like plastics, rubbers, etc. UV protection, flame retardancy, and weathering resistance are very important for wood based composites used in exterior applications.

In polymer composite, ZnO nanopowder is one of the widely used filler. ZnO enhances the thermal, mechanical, UV resistance, as well as other relevant properties of the composite.[8–10] Polymer-ZnO composites have been explored as technological important due to their potential applications in solar cells, electrochromic windows, optical device, gas sensing, and in antimicrobial application of food preservation.[11–14] Reports based on wood/polymer/clay nanocomposite are available in literature. However, far less is known regarding wood polymer nanocomposite by using both clay and metal oxide. It is envisaged that a thorough study may provide some valuable information for the development of WPC in future.

This study is aimed to discuss the effect of ZnO nanopowder along with nanoclay to the thermal and mechanical properties of HDPE/LDPE/PP/PVC blend/wood/nanoclay composite. The aim is also to study the effect of ZnO to other properties like UV resistance, flame retardancy, and water uptake of the composites.

EXPERIMENTAL

Materials

HDPE and LDPE (Grade: PE/20/TK/CN) were collected from Plast Alloys India Ltd. (Harayana, India). PP homopolymer (Grade: H110MA, MFI 11g/10 min) was collected from Reliance Industries Ltd. (Mumbai, India). PVC (Grade: SPVC FS: 6701) was collected from Finolex Industries Ltd. (Pune, India). The compatibilizer, polyethylene-*co*-glycidyl methacrylate (PE-*co*-GMA; Otto chemicals, Mumbai, India), *N*-Cetyl-N,N,*N*-trimethyl ammonium bromide (CTAB; Central Drug house (P) Ltd., Delhi, India), nanomer (clay modified by 15–35 wt % octadecylamine and 0.5–5 wt % aminopropyltriethoxy silane, ζ-Aldrich, USA), and ZnO nanopowder (<100 nm; Aldrich, Germany) were used as received. A nonconventional wood, nal (*Phragmites karka*) was collected from local forest of Assam. Other reagents used were of analytical grade.

Preparation of wood samples

Nal (*P. karka*) is a kind of softwood available in the forest of Assam. It was collected and chopped into small strips. These strips were initially washed with 1% soap solution. It was followed by washing with 1% NaOH solution and finally washed with cold water. The washed wood strips were oven dried at 100 ± 5°C till attainment of constant weight. These dried wood strips were grinded in a mixer, sieved at about 60 mesh size, and kept for subsequent use.

Modification of ZnO

The surface of ZnO nanoparticles was modified with cationic surfactant CTAB to improve its miscibility with the hydrophobic polymers. Approximately 10 g of ZnO was taken in a round bottom flask containing 1:1 ethanol–water mixture. It was fitted with spiral condenser and stirred at 80°C for 24 h. Then 12 g of CTAB was taken in a beaker containing ethanol–water mixture and stirred at 80°C for 6 h. This mixture was added to ZnO mixture and finally stirred for another 24 h. The mixture was then filtered and washed with deionized water for several times. It was collected and dried overnight in vacuum oven at 45°C. After completion of drying, the mixture was grinded and stored in desiccator to avoid moisture absorption. The presence of long organic chain of cetyl group and the surface hydroxyl group of modified ZnO would enhance the interaction between ZnO, polymers, wood, and clay.

Preparation of wood polymer nanocomposite

Approximately 6 gram each of HDPE, LDPE, and PP (1 : 1 : 1) were added slowly to 105 mL of xylene taken in a flask fitted with a spiral condenser at room temperature. This was followed by the addition of the PE-*co*-GMA (5 phr). The temperature of the flask was increased to 130°C to make a homogenous solution. Now, another solution containing 3 g of PVC in 35 mL of tetrahydrofuran (THF) was prepared. The temperature of the previous polymer solution was decreased to 120°C. The PVC solution was then mixed with the other polymer solution at 120°C (approximately) under stirring condition for 1 h. A known quantity of nanoclay (3 phr) and CTAB modified ZnO nanopowder (1–5 phr) was dispersed in 15 mL of THF solution using stirrer and sonication. This dispersed mixture was added gradually to the polymer solution under stirring condition. Oven

dried WF (40 phr) was added slowly to this mixture and stirred for another 1 h. It was transferred in tray, dried, and grinded. The composite sheets were obtained by the compression molding press (Santec, New Delhi) at 150°C under a pressure of 80 MPa.

Polymer blend (HDPE + LDPE + PP + PVC), Polymer blend/5phr PE-*co*-GMA, and polymer blend/5 phr PE-*co*-GMA/40 phr wood were designated as PB, PB/G5, and PB/G5/W40. The 1, 3, and 5 phr ZnO filled WPC containing 3 phr nanoclay were designated as PB/G5/W40/N3/Z1, PB/G5/W40/N3/Z3, and PB/G5/W40/N3/Z5.

Measurements

XRD study

The degree of intercalation of nanoclay and distribution of ZnO in WPC was examined by X-ray diffractometry. It was carried out in a Rigaku X-ray diffractometer (Miniflax, UK) using CuKα ($\lambda = 0.154$ nm) radiation at a scanning rate of 1° per minute with an angle ranging from 2° to 70°.

TEM study

The dispersion of the silicate layers of nanoclay and ZnO nanoparticles in WPCs was performed by using transmission electron microscopy (TEM; JEM-100 CX II) at an accelerated voltage of 20–100 kV.

SEM study

The compatibility among different polymers as well as morphological features of the WPC was studied by using scanning electron microscope (JEOL JSM - 6390LV) at an accelerated voltage of 5–10 kV. Fractured surface of the samples, deposited on a brass holder and sputtered with platinum, were used for this study.

FTIR studies

FTIR spectra of WF, ZnO nanopowder, and WPC loaded with nanoclay and ZnO nanopowder were recorded in Fourier Transform Infrared spectrophotometer (Impact-410, Nicolet, USA) using KBr pellet.

Mechanical property study

The tensile and flexural tests for polymer blend, PE-*co*-GMA treated polymer blend, and WPC loaded with different percentage of ZnO were carried out using Universal Testing Machine (Zwick, model Z010) at a crosshead speed of 10 mm min^{-1} at room temperature according to ASTM D-638 and D-790, respectively. A total of 10 samples of each category were tested and their average values were reported.

Hardness study

The hardness of the samples was measured according to ASTM D-2240 using a durameter (model RR12) and expressed as shore D hardness.

Thermal property study

Thermal properties of polymer blend and the WPCs were measured in a thermogravimetric analyzer (TGA-50, shimadzu) at a heating rate of 10°C min^{-1} up to 600°C under nitrogen atmosphere.

UV resistance test

The degradation study of the WPC samples was done in UV chamber (Model: S.L.W, voltage: 230 V; Advanced Research Co., India) using a mercury arc lamp system that produces a collimated and highly uniform UV flux in the 254–365 nm range. Specimen's dimensions of $25 \times 25 \times 5$ mm^3 were exposed in the UV chamber at room temperature and characterized at specified time intervals. The weight loss was measured and is expressed as follows[15]:

$$\%\text{weightloss} = (W_t - W_o/W_o) \times 100$$

where, W_t is the specimen weight at time t and W_o is the specimen weight before exposure. Surface morphology of UV degraded specimen was characterized by scanning electron microscopy (SEM). Chemical degradation was studied by FTIR. The intensity of the carbonyl (C=O) stretching peaks at 1715 cm^{-1} in cellulose of WF was measured. The net peak heights were determined by subtracting the height of the baseline directly from the total peak height. The same base line was taken for each peak before and after exposure to UV.[16] The carbonyl index was calculated by using the following equation:

$$\text{Carbonyl index} = I_{1715}/I_{2912}(100)$$

where, I represent the intensity of the peak. The peak intensities were normalized by using —CH stretching peak of alkane at 2912 cm^{-1}. This peak was chosen as reference due to its least change during irradiation.

LOI study

WPC samples were cut into the dimensions of $100 \times 10 \times 5$ mm^3 for limiting oxygen index (LOI) test by using flammability tester (S.C. Dey Co., Kolkata) according to ASTM D-2863 method.[17] The total volume of the gas mixture ($N_2 + O_2$) was kept fixed at 18 cc. The volume of nitrogen gas and that of oxygen gas were kept initially at a maximum and minimum level. Now, the volume of nitrogen gas was decreased and

that of oxygen gas was increased gradually. However, the total volume of gas mixture was kept fixed at 18 cc during the experiment. The sample was placed vertically in the sample holder of the LOI apparatus. The ratio of nitrogen and oxygen at which the sample continued to burn for at least 30 s was recorded.

$$\text{Limiting oxygen index (LOI)} = \text{Volume of } O_2/\text{Volume of } (O_2 + N_2)100.$$

Water uptake and water vapor exclusion study

WPC samples were cut into 2.5 × 0.5 × 2.5 cm^3 for water uptake and water vapor exclusion study. Percentage water uptake was measured by submerging the samples in distilled water at room temperature (30°C) for different time periods after conditioning at 65% relative humidity and 30°C and expressed according to the formulae,

$$\text{Water uptake}\,(\%) = (W_s - W_1)/W_1 \times 100$$

where, W_s is the weight of the water saturated sample and W_1 is the weight of the oven dried sample.

The water vapor exclusion test was carried out at 65% relative humidity and 30°C. Weights of the samples were measured after 12, 24, 36, 48, 60, and 72 h. The samples were oven dried and conditioned at 30°C and 30% relative humidity before the test. It is expressed as a percentage of moisture absorbed based on oven dry weight.

RESULTS AND DISCUSSION

XRD results

Figure 1 shows the X-ray diffraction (XRD) results of nanoclay, polymer blend, ZnO, and WPC loaded with clay (3 phr) and different percentage of ZnO (1–5 phr). Organically modified nanoclay (curve-a) shows the diffraction peak at 2θ = 4.11° with basal spacing 2.15 nm. Curve-b represents the diffractrogram of polymer blend. The most prominent wide-angle XRD peaks appeared at 2θ = 14.12, (200) 17.06, (040) 18.64, (211) 21.62 (110), and 24.02 (200) were for crystalline portion of different polymers present in the blend.[18–21] The crystalline peaks appear above 2θ = 30° (shown in curve-c) were the characteristic peaks of ZnO nanopowder.[22] Curve (*d*–f) was for WPC loaded with nanoclay (3 phr) and different percentage of ZnO (1–5 phr). The diffractograms of composites did not exhibit any characteristic peak of nanoclay. It could be said that either an exfoliation or increase in disorder in nanoclay occurred which was not possible to detect by XRD analysis. The crystalline peak intensity of the polymer blend appeared in the range 2θ = 14–25° was found to decrease with the increase in the level of incorporation of ZnO (1–5 phr). However, the intensities of peak corresponding to ZnO nanopowder increased with the increase in the concentration of ZnO in the composite. Similar decreased in peak intensities of polymer and increase of peak intensity of TiO_2 was observed and reported by Mina et al.[18] while studying the XRD profile of PP /titanium dioxide composite. It could be concluded that nanoclay layers were disordered and ZnO particles were incorporated in the wood polymer matrix.

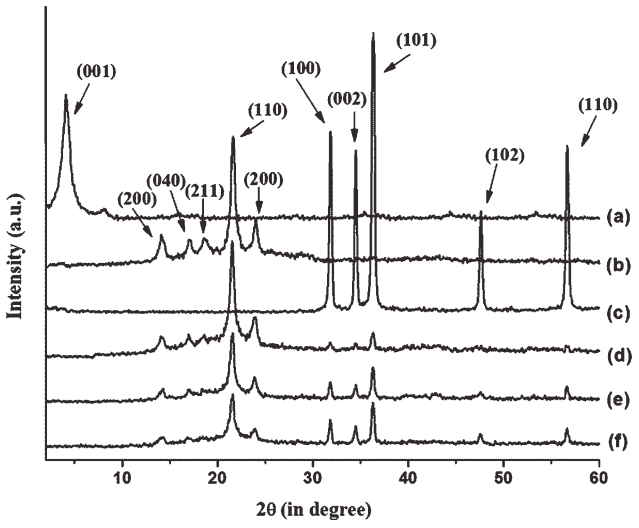

Figure 1 XRD of (a) Nanoclay, (b) PB, (c) nano ZnO, (d) PB/G5/W40/N3/Z1, (e) PB/G5/W40/N3/Z3, and (f) PB/G5/W40/N3/Z5.

TEM results

Figure 2 shows the TEM micrographs of WPC loaded with nanoclay (3 phr) and different percentage of ZnO (1–5 phr). The dark slices (arrow marked) represent the layers of nanoclay while the dark spots (arrow marked) are for ZnO nanoparticles. The distribution of ZnO (1–3 phr) was better in the WPC compared with that of composite containing higher proportion (5 phr) of ZnO [ig. 2(c)]. Kim et al.[23] prepared PAN/ZnO nanocomposite and found that ZnO nanoparticles were well dispersed within the composite. At higher concentration of ZnO, the distances between ZnO particles became less and this might have enhanced the tendency for agglomeration.

SEM study

Figure 3 shows the SEM micrographs of polymer blend with and without compatibilizer, WPC and WPC loaded with nanoclay, and different percentage of ZnO nanopowder. The fractured surface of some selective samples was considered for this study. The polymer mixtures were immiscible as judged by separation of different phases [Fig. 3(a)]. The miscibility

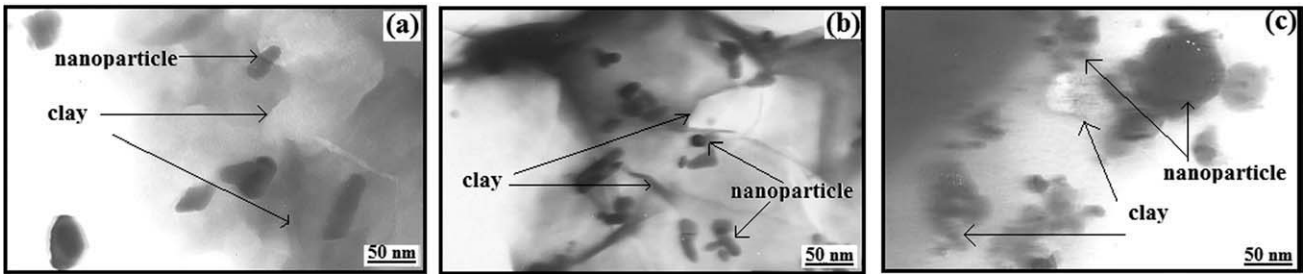

Figure 2 TEM micrographs of (a) PB/G5/W40/N3/Z1, (b) PB/G5/W40/N3/Z3, and (c) PB/G5/W40/N3/Z5.

improved due to addition of PE-*co*-GMA as compatibilizer [Fig. 3(b)]. The compatibilizer enhanced the interfacial adhesion among the polymers through its long hydrocarbon chain and epoxy group which resulted in an improvement in miscibility. The use of ethylene–glycidyl methacrylate for improving the adhesion between polyolefins and PET was reported in the literature.[24] The addition of WF decreased the roughness of fractured surface of the composite [Fig. 3(c)]. The roughness of the fractured surface decreased further after the incorporation of WF, clay, and ZnO to the polymer blend [Fig. 3(d–e)]. The fractured surface of composite having nanoclay and 3 phr ZnO appeared to be smoother compared with those of composite prepared with either 1 or 5 phr ZnO and nanoclay. This might be due to the improvement in interaction among PE-*co*-GMA, nanoclay, ZnO, polymer, and wood. The decrease in smoothness at higher concentration of ZnO was due to the aggregation of ZnO. Similar observation was reported by He et al.[25] during study of the morphology of PET/ZnO nanocomposite.

FTIR study

FTIR spectra of CTAB, ZnO, and CTAB modified ZnO are shown in Figure 4. In the spectrum of CTAB [Fig. 4(a)], the absorption peaks at 2918, 2848, and 1475 cm^{-1} were assigned to asymmetric, symmetric stretching, and scissor modes of —CH_2 in the methylene chains, respectively.[26] FTIR spectrum of unmodified ZnO nanoparticles is presented in Figure 4(b). Absorption peaks at 3438 and 1633 cm^{-1} in the spectra was due to —OH (-stretching) and —OH (-bending) vibrations while the peaks around 420 cm^{-1} was due to the vibration of metal–oxygen (M–O) bond as reported in the literature.[27] The FTIR spectrum of ZnO modified with CTAB is represented by the curve 4c. It was observed that the intensity of the peak for —OH group decreased to

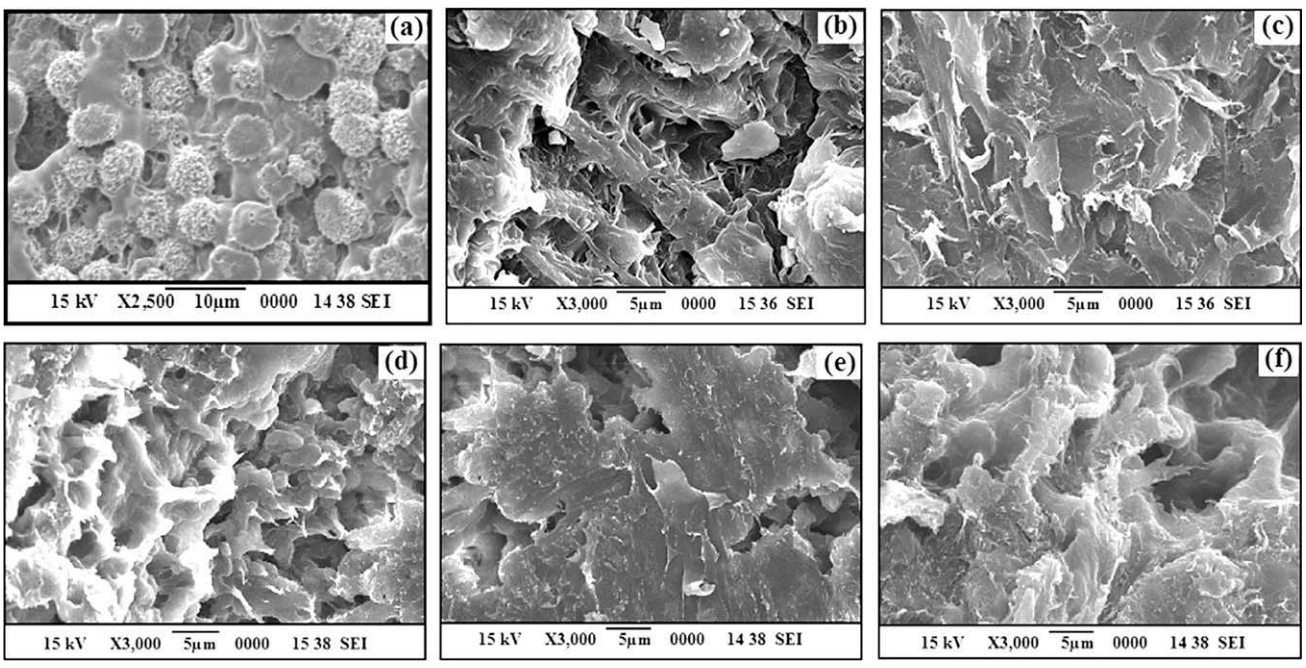

Figure 3 SEM micrographs of (a) PB, (b) PB/G5, (c) PB/G5/W40, (d) PB/G5/W40/N3/Z1, (e) PB/G5/W40/N3/Z3, and (f) PB/G5/W40/N3/Z5.

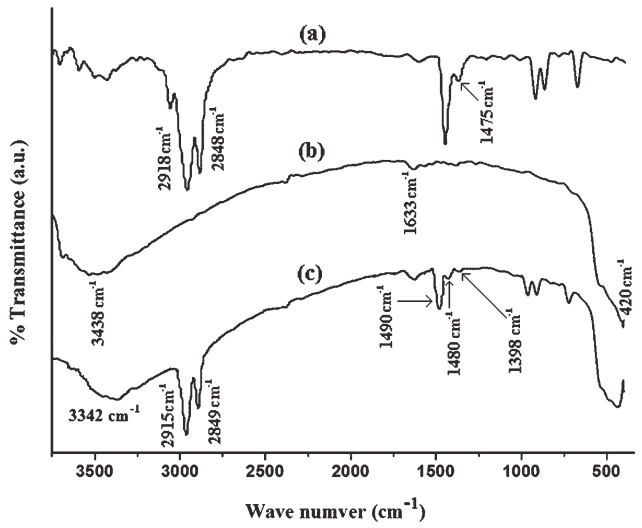

Figure 4 FTIR spectra of (a) CTAB, (b) unmodified ZnO nanopowder, and (c) CTAB modified ZnO.

wave number 3342 cm^{-1}. Besides this, two new peaks at 2915 and 2849 cm^{-1}, which were due to the presence of —CH_2 group of CTAB were appeared in the spectrum. The peaks at 1490 and 1480 cm^{-1} were due to the asymmetric CH_3-N^+ deformation mode of the CTAB head group. Another peak present at 1398 cm^{-1} was due to the symmetric CH_3—N^+ deformation mode of CTAB head group.[26] These results indicated that long chain of CTAB group had been incorporated on the surface of the ZnO nanoparticles. Furthermore, CTAB modified ZnO was dispersed in a flask containing xylene and kept for checking of any settling of particles. The dispersion of ZnO was found to be stable. This indicated that proper modification occurred.

Figure 5 shows the FTIR spectra of wood, nanoclay, WPC excluding nanoclay and ZnO, and WPC containing nanoclay with different percentage of ZnO. Curve-a representing the wood sample shows the presence of bands at 3436 cm^{-1} for —OH stretching, 2932 and 2849 cm^{-1} for —CH stretching, 1732 cm^{-1} for C=O stretching, 1639 cm^{-1} for —OH bending, 1161 and 1045 cm^{-1} for C—O stretching, and 1000–650 cm^{-1} for C—H bending vibration (out of plane). Organically modified nanoclay (curve b) exhibits the peaks at 3470 cm^{-1} (—OH stretching) 2935 and 2852 cm^{-1} (—CH stretching of modified hydrocarbon), 1621 cm^{-1} (—OH bending), and 1032–461 cm^{-1} (oxide bands of metals like Si, Al, Mg, etc.).[28] PB/G5/W40 (curve c) shows peaks at 2923 cm^{-1} (—CH stretching), 1734 cm^{-1} (C=O stretching), 1636 cm^{-1} (—OH bending), and 720 cm^{-1} (—CH_2 stretching).

Figure 5(d–f) represents the FTIR spectra of WPC loaded with 3 phr nanoclay and 1, 3, and 5 phr of ZnO. From the figure, it was observed that the intensity of —OH stretching was decreased and shifted to 3434 cm^{-1} (curve-d), 3419 cm^{-1} (curve-e), and 3430 cm^{-1} (curve-f) from 3436 cm^{-1} (wood). The decrease in peak intensity of —OH stretching might be ascribed to the participation of hydroxyl group of clay and ZnO in the crosslinking reaction with wood and polymer. The shifting of hydroxyl absorption peak to lower wave number was due to the formation of hydrogen bond between WF and polymer. A similar decrease in intensity of —OH absorption peak and shifting to lower wavelength was reported by Deka and Maji [29] while studying the FTIR spectra of nanoclay treated WPC. Dhoke et al.[27] studied the interaction between nano-ZnO particles and alkyd resin by FTIR technique. A significant decrease in peak intensity of hydroxyl group of alkyd resin was observed. The intensity of —CH stretching peaks at 2932 cm^{-1} and 2848 cm^{-1} (curve *d*–f) was found to increase. Similar increase in —CH peak intensities was observed by Awal et al.[30] The peak intensities (1032–461 cm^{-1}) of metal oxides bond of nanoclay and ZnO (curve *d*–f) was decreased to a considerable extent. Moreover, the flexural and tensile properties of the composites improved due to incorporation of clay and ZnO as explained later. All these suggested a strong interaction between wood, nanoclay, ZnO, and polymer.

Mechanical property

Table I shows the flexural and tensile properties of polymer blends and WPC loaded with nanoclay and different percentage of ZnO nanopowder. From the table, it was observed that both flexural and tensile properties of the polymer blend increased after incorporation of compatibilizer. The compatibilizer

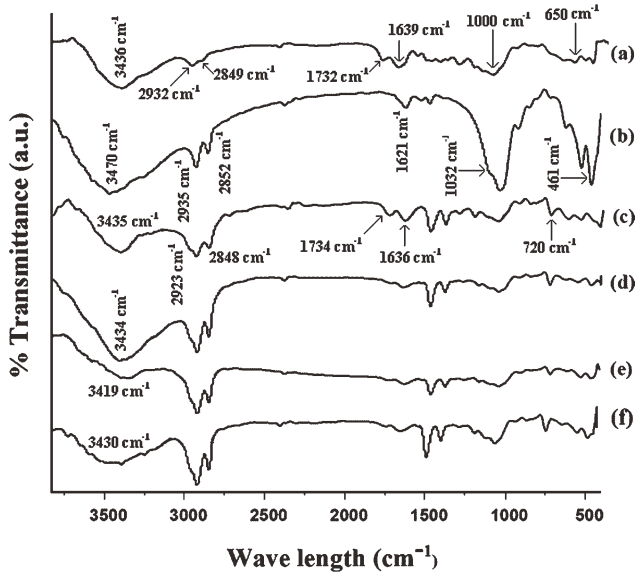

Figure 5 FTIR spectra of (a) wood, (b) nanoclay, (c) PB/G5/W40, (d) PB/G5/W40/N3/Z1, (e) PB/G5/W40/N3/Z3, and (f) PB/G5/W40/N3/Z5.

TABLE I
Flexural, Tensile and Hardness Properties of Polymer Blend and WPC Loaded with Nanoclay and Different Percentage of ZnO

Sample	Flexural properties		Tensile properties		Hardness
	Strength (MPa)	Modulus (MPa)	Strength (MPa)	Modulus (MPa)	(Shore D)
PB	12.34 ± 0.36	756.41 ± 1.28	5.87 ± 1.21	85.42 ± 16.23	66.7 (± 0.3)
PB/G5	15.34 ± 1.08	1026.32 ± 1.07	9.04 ± 1.16	113.54 ± 17.23	68.4 (± 0.5)
PB/G5/W40	17.13 ± 1.11	3756.18 ± 1.15	17.82 ± 1.21	254.84 ± 18.26	66.8 (± 0.7)
PB/G5/W40/N3/Z1	28.14 ± 0.72	4843.81 ± 1.31	32.28 ± 1.47	603.45 ± 17.25	74.3 (± 0.2)
PB/G5/W40/N3/Z3	31.79 ± 1.12	5052.58 ± 1.36	35.65 ± 1.56	657.32 ± 17.16	79.4 (± 0.2)
PB/G5/W40/N3/Z5	29.25 ± 1.71	4927.41 ± 1.29	30.24 ± 1.14	629.87 ± 18.74	77.1 (± 0.3)

improved the interfacial adhesion between the polymers due to which both flexural and tensile properties increased. The flexural and tensile properties of the composite were further improved after the addition of WF. The WF acted as a load carrier, reinforced the composites, and increased the flexural and tensile properties. Salemane and Luyt[31] prepared wood/PP composite and found an improvement in mechanical properties due to reinforcement by WF. Moreover, the compatibilizer, PE-*co*-GMA, increased the interfacial adhesion between wood and polymers through its glycidyl linkage and long polymeric chain. Sailaja[32] used poly(ethylene-*co*-glycidyl methacrylate) as compatibilizer to improve the compatibility of wood pulp-LDPE composite. The properties were further improved after the incorporation of clay and ZnO nanopowder. At a fixed clay loading (3 phr), both the flexural and tensile properties improved upto addition of 3 phr of ZnO. The properties decreased on addition of higher amount of ZnO (5 phr). The observed higher values might be due to the combined effect of nanoclay and ZnO. The silicate layers of nanoclay acted as a reinforcing agent that binds the polymer chain inside the gallery space and hence restrict the mobility of the polymer chain. The incorporation of clay increased the mechanical properties of wood-plastic composite was reported.[33] CTAB modified ZnO improved the interaction between clay, wood, and polymer through its surface hydroxyl group and cetyl group, respectively. The higher the dispersion of ZnO, the higher would be the interaction. At higher level of ZnO loading (5 phr), the agglomeration occurred, and hence the interaction of ZnO with the clay, polymer, and wood decreased. The interaction of ZnO nanoparticles increased the tensile modulus of polyacrylonitrile was reported in the literature.[23]

Hardness results

Table I shows the hardness results of polymer blend and WPC loaded with clay and different percentage of ZnO. Hardness value of the polymer blend increased after the addition of compatibilizer due to enhancement of interfacial adhesion between polymers. On addition of WF to the polymer blend, the hardness value was found to decrease. But after the incorporation of nanoclay and ZnO to the WPC, hardness value was found to increase again. The improvement was due to combined effect of increase in interaction of clay and ZnO with WF and polymer. Hardness value was found maximum at 3 phr of clay/ZnO loading, after that it decreased. At higher loading of ZnO, the reinforcing action of ZnO might decrease due to agglomeration.

Thermogravimetric analysis

Table II shows the initial decomposition temperature (T_i), maximum pyrolysis temperature (T_m),

TABLE II
Thermal Analysis of Polymer Blend and Wood Polymer Nanocomposite Loaded with Clay and Different Percentage of ZnO

Sample	T_i	T_m[a]	T_m[b]	Temperature of decomposition (T_D) in °C at different weight loss (%)				RW% at 600°C
				20%	40%	60%	80%	
PB	249	270	407	291	388	439	468	6.1
PB/G5/W40	255	276	451	299	397	446	473	7.2
PB/G5/W40/N3/Z1	277	326	503	330	459	484	501	10.8
PB/G5/W40/N3/Z3	289	337	517	350	478	497	513	14.5
PB/G5/W40/N3/Z5	281	330	510	336	465	490	508	12.7

T_i, value for initial degradation.
[a] T_m, value for first step
[b] T_m, value for second step.

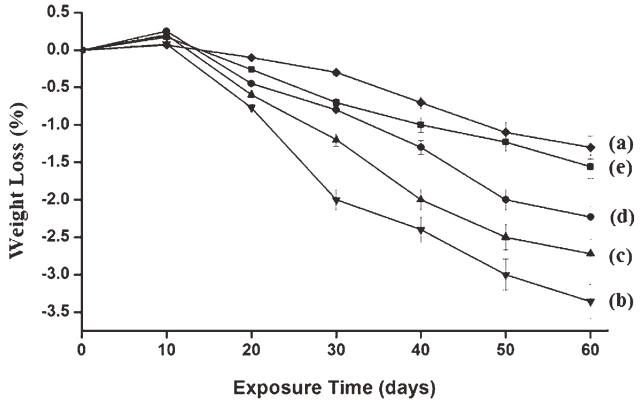

Figure 6 Weight losses versus exposure time of (a) PB, (b) PB/G5/W40, (c) PB/G5/W40/N3/Z1, (d) PB/G5/W40/N3/Z5, and (e) PB/G5/W40/N3/Z3.

decomposition temperature at different weight loss (%; T_D), and residual weight (RW, %) for polymer blend and WPCs. It was observed that T_i value increased after the incorporation of compatibilizer and WF to polymer blend. The value increased further after the addition of nanoclay and ZnO. T_i value was found maximum when the concentration of ZnO was 3 phr. At higher concentration of ZnO, the T_i value decreased again.

Both the polymer blend and composite showed two decomposition peaks. The T_m value for the first step in both WPC and WPC loaded with clay and ZnO were due to the depolymerization of hemicellulose, glycosidic linkage of cellulose, thermal decomposition of cellulose,[34] and dehydrochlorination of PVC while the peak for second step was due to decomposition of HDPE and PP.[35–37] T_m values of the composites for both the steps were found to follow the similar trend as those of T_i values.

The percentage weight losses of sample at different temperature are listed in Table II. WPC containing 3 phr nanoclay and 3 phr ZnO exhibited similar weight losses at higher temperatures compared to polymer blend, WPC, and WPC containing 1 or 5 phr ZnO.

The incorporation of compatibilizer enhanced the interaction between the polymer blend and WF. The improvement of thermal stability after inclusion of compatibilizer and WF to polymer blend was reported by Awal et al.[30] The silicate layers of nanoclay in nanocomposites provided a long tortuous path which delayed the diffusion of the decomposed volatile product through the composite. Deka and Maji [29] reported that thermal stability of WPC enhanced due to addition of clay. Moreover, the incorporation of modified ZnO nanopowder might play a role in enhancing the thermal stability by interacting with clay, wood and polymer through its surface hydroxyl group and cetyl groups, respectively. At higher concentration of ZnO, the agglomeration (as evident by TEM study) probably decreased the interaction and could give rise to reduce the thermal stability. Laachachi et al.[38] studied the thermal degradation of PMMA by incorporation of ZnO and organo-modified montmorillonite and found an increased in thermal stability of polymethyl methacrylate after the incorporation of ZnO and organo-montmorillonite.

UV test results

Figure 6 displays the weight loss of polymer blend, normal WPC and WPC loaded with nanoclay and ZnO (1–5 phr). Weight losses of the samples were determined as a function of exposure time at room temperature and were found nearly linear with exposure time. At early stage of exposure time, due to moisture uptake, a small increase of weight was found, which was greater than the material loss induced by the degradation in the early stage. The rate of weight loss was lowest for polymer blend followed by WPC filled with 3 phr ZnO and 3 phr clay, 5 phr ZnO and 3 phr clay, as well as 1 phr ZnO and 3 phr clay. WPC showed the maximum weight losses. After 60 days of exposure, the maximum weight losses in polymer blend, normal WPC and clay loaded 1, 3, and 5 phr ZnO containing WPCs were 1.3% ± 0.2%, 3.3% ± 0.2%, 2.7% ± 0.2%, 1.5% ± 0.3%, and 2.2% ± 0.5%, respectively. On exposure to UV radiation, the chain scission followed by decrease in the density of the entanglements of the polymer chains occurred. This resulted in the decrease in the weight of the samples.

Figure 7 shows the carbonyl index values against time. After irradiation of the samples for 60 days, carbonyl peak intensity was found to increase (Fig. 8). On exposing the samples to UV radiation, chain scission of the polymer blend occurred that increased the carbonyl index value. The polymer blend had lowest carbonyl index value (curve-7a).

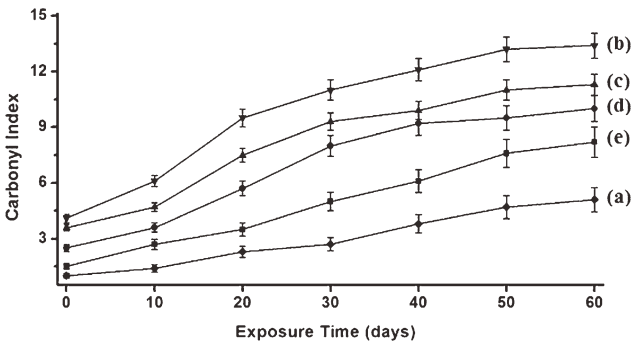

Figure 7 Carbonyl index value of (a) PB, (b) PB/G5/W40, (c) PB/G5/W40/N3/Z1, (d) PB/G5/W40/N3/Z5, and (e) PB/G5/W40/N3/Z3.

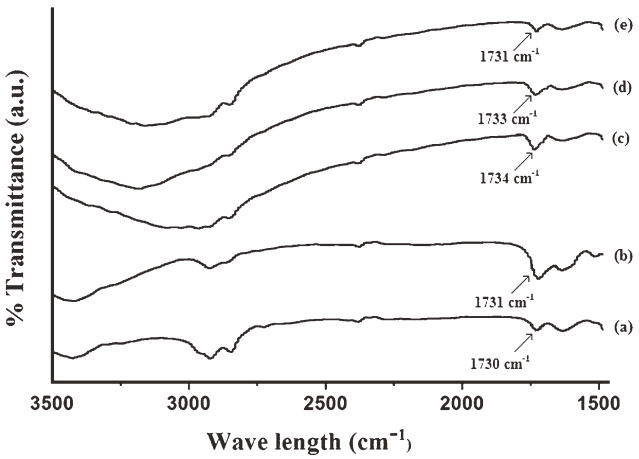

Figure 8 Change in carbonyl peak intensity of (a) PB, (b) PB/G5/W40, (c) PB/G5/W40/N3/Z1, (d) PB/G5/W40/N3/Z5, and (e) PB/G5/W40/N3/Z3.

Due to higher oxidation of WF, normal WPC had highest carbonyl index value (curve-7b). The carbonyl index values decreased upto the addition of 3 phr clay and ZnO after that it increased. ZnO nanoparticles played an important role in stabilizing the WPC by acting as screen and delayed the photodegradation process. ZnO nanoparticles absorbed the UV radiation and hence reduced the UV intensity required for the oxidation of the WPC. Zhao and Li[39] observed an improvement in UV stability of PP nanocomposite due to the incorporation of ZnO. The presence of nanoclay in the composite also had a screening effect that delayed the photo degradation process. Grigoriadou et al.[40] observed an increase in UV stability of HDPE after incorporating montmorillonite clay. Figure 9 represents the SEM micrographs of samples after 60 days of irradiation. The surface morphology of the samples showed a drastic change due to exposure to UV radiation. The surface of normal WPC was more irregular compared with clay/ZnO treated WPC indicating that the normal WPC sample was less effective compared with ZnO/clay containing sample against UV radiation. WPC containing nanoclay and higher percentage of ZnO (5 phr) exhibited lower protection against UV radiation as shown by the decrease in surface smoothness compared to WPC loaded with 3 phr ZnO and nanoclay. This might be due to the agglomeration of ZnO which provided lower protection against photodegradation.

LOI results

LOI values of polymer blend, WPC, and WPC loaded with nanoclay and ZnO are shown in Table III. From the table, it was observed that with the addition of compatibilizer, LOI value of the polymer blend increased. The increase in the value was due to the increase in interfacial adhesion among the polymers by the compatibilizer. LOI value increased further after the addition of WF to the blend. The glycidyl and hydrocarbon part of the compatibilizer improved the interaction with the hydroxyl and hydrocarbon part of the wood and polymer. A

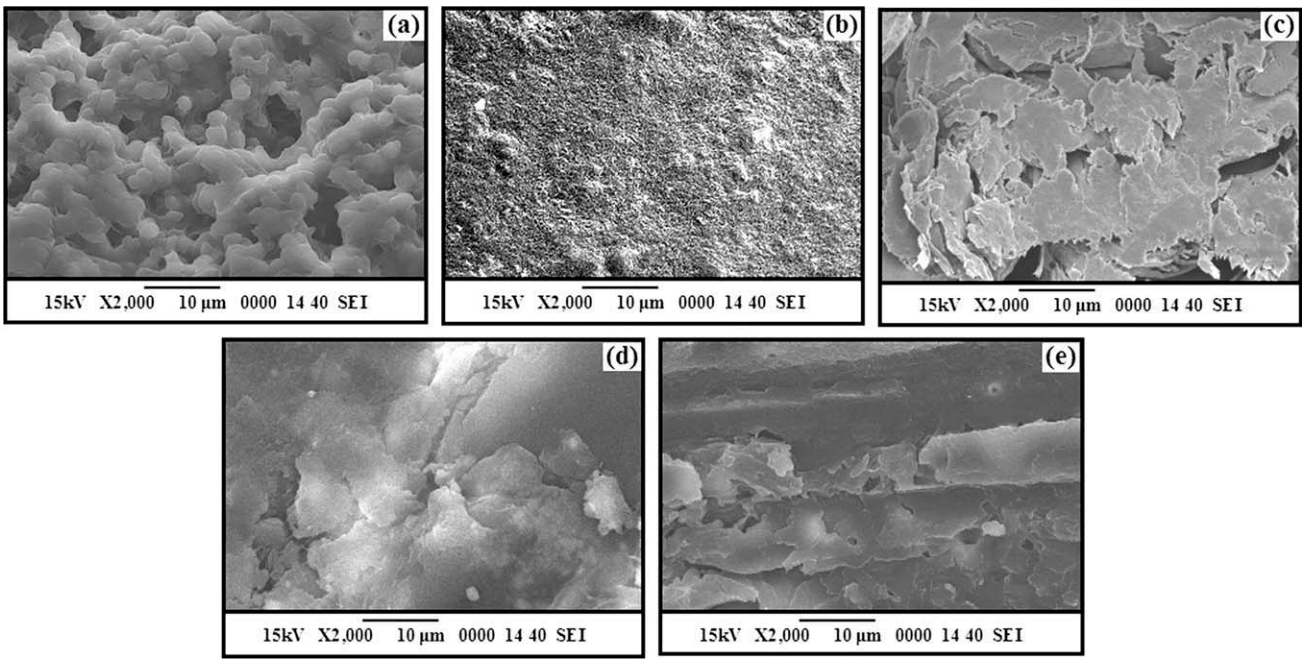

Figure 9 SEM micrographs of UV treated samples after 60 days: (a) PB, (b) PB/G5/W40, (c) PB/G5/W40/N3/Z1, (d) PB/G5/W40/N3/Z3, and (e) PB/G5/W40/N3/Z5.

TABLE III
LOIs and Flaming Characteristics of Polymer Blend and Wood/Polymer/Clay/ZnO Nanocomposites

Samples	LOI (%)	Flame description	Smoke and Fumes	Char
PB	20	Candle-like localized flame	Small and black smoke	little
PB/G5	35	Small localized flame	Small and black smoke	little
PB/G5/W40	38	Small localized flame	Small and black smoke	little
PB/G5/W40/N3/Z1	53	Small localized flame	Small and black smoke	higher
PB/G5/W40/N3/Z3	68	Small localized flame	Small and black smoke	higher
PB/G5/W40/N3/Z5	66	Small localized flame	Small and black smoke	higher

substantial improvement in LOI value was observed after the addition of clay and ZnO. The value increased upto the addition of 3 phr each of nanoclay and ZnO. LOI value decreased at higher concentration of ZnO (5 phr). The nanoclay produced silicate char on the surface of WPC which increased the flame resistance property of the composite.[41] The tortuous path provided by the silicate layers had better barrier property to the oxygen and heat which delayed the burning capacity of the composite. The incorporation of CTAB modified ZnO enhanced the interaction between clay, wood, and polymer through its hydroxyl and cetyl groups. ZnO nanoparticles also provided some thermal barrier to the oxygen and heat leading to an improvement in flame resistant property. At higher ZnO loading, the agglomeration of ZnO resulted in decrease of interaction and hence barrier property as well as LOI value.

Water uptake and water vapor exclusion results

The water uptake and water vapor uptake results of polymer blend, PE-*co*-GMA treated polymer blend, and WPC loaded with clay and different percentage of ZnO are shown in Figure 10. The water uptake capacity of polymer blend decreased after the addition of PE-*co*-GMA compatibilizer. The decreased in water uptake capacity of PE-*co*-GMA treated polymer blend was due to the increase in interfacial adhesion between the polymers by the compatibilizer. The value of water uptake capacity was suddenly increased after the addition of WF to the blend. The hydrophilic nature of WF caused an increase in the water uptake capacity. The water uptake capacity was decreased after the addition of clay/ZnO. WPC loaded with 3 phr each of clay and ZnO showed lowest water uptake capacity followed by WPC with 3 phr clay and 1 phr ZnO, and WPC with 3 phr clay and 5 phr ZnO. The silicate layers of the clay provided tortuous path and increased the barrier property for water transport.[29] ZnO nanopowder also provided a barrier to the passage of water. Better the distribution of nanoparticles, the higher was the barrier property. ZnO nanoparticles at higher concentration were found to become agglomerated in the composite which resulted in an increase in water uptake capacity.

Water vapor exclusion test for the samples were carried out at 30°C and 65% relative humidity. The water vapor uptake was found to increase with time. The trend and explanation for water vapor absorption of different samples were similar to those of samples taken for water uptake study.

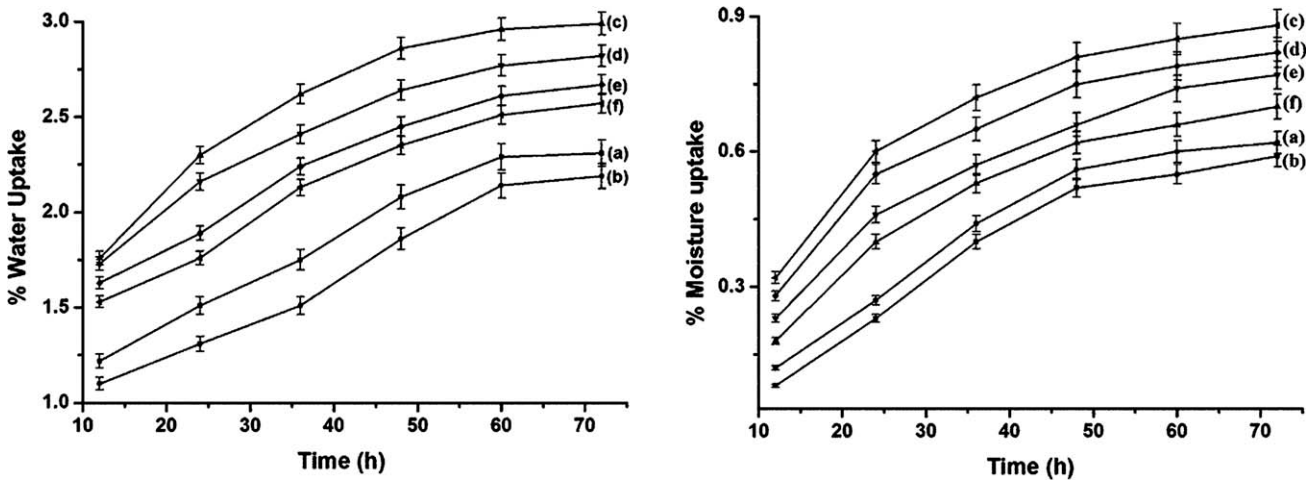

Figure 10 Water absorption and Water vapor absorption of (a) PB, (b) PB/G5, (c) PB/G5/W40, (d) PB/G5/W40/N3/Z1, (e) PB/G5/W40/N3/Z5, and (f) PB/G5/W40/N3/Z3.

CONCLUSIONS

The optimized ratio of xylene and THF for solution blending of HDPE, LDPE, PP, and PVC (1 : 1 : 1: 0.5) was 70 : 30. The compatibility among the polymers and WF was improved by using PE-*co*-GMA compatibilizer as revealed by SEM study. The distribution of silicate layers of nanoclay and ZnO in WPCs were examined by XRD and TEM study. Surface modification of ZnO nanoparticles by cationic surfactant CTAB was examined by FTIR studies. The interactions among wood, PE-*co*-GMA, ZnO, and nanoclay were also studied by FTIR. WPC loaded with nanoclay and ZnO showed an improvement in mechanical and thermal properties. The incorporation of ZnO improved the UV resistance of the composites as judged from the decrease in weight loss, carbonyl index value and SEM study. Nanoclay/ZnO treated WPC further improved the flame retardancy and decreased the water absorption capacity. WPC loaded with 3 phr clay and 3 phr ZnO exhibited maximum improvement in properties.

The authors thank Council of Scientific and Industrial Research (CSIR), New Delhi, for their financial assistance (grant number: 01(2287)/08/EMR-II).

References

1. Selke, S. E.; Wichman, I. Compos Part A: Appl Sci 2004, 35, 321.
2. Ashori A. Bioresour Technol 2008, 99, 4661.
3. Ashori, A.; Nourbakhsh, A. Bioresour Technol 2010, 101, 2515.
4. Qiu, W.; Zhang, F.; Endo, T.; Hirotsu, T. Polym Compos 2005, 26, 448.
5. Devi, R. R.; Maji, T. K. Polym Compos 2007, 28, 1.
6. Biswal, M.; Mohanty, S.; Nayak, S. K. J Appl Polym Sci 2009, 114, 4091.
7. Song, G. J Mater Rep 1996, 4, 57.
8. Liufu, S. C.; Xiao, H. N.; Li, Y. P. Polym Degrad Stab 2005, 87, 103.
9. Demir, M. M.; Memesa, M.; Castignolles, P.; Wegner, G. Macromol Rapid Commun 2006, 27, 763.
10. Lu, N.; Lu, X.; Jin, X.; Lu, C. Polym Int 2007, 56, 138.
11. Ji, L. W.; Shih, W. S.; Fang, T. H.; Wu, C. Z.; Peng, S. M.; Meen, T. H. J Mater Sci 2010, 45, 3266.
12. Zhang, H.; Wu, J.; Zhai, C; Du, N; Ma, X; Yang, D. Nanotechnology 18: 455604 2007.
13. Jin, T.; Sun, D.; Su, J. Y.; Zhang, H; Sue, H. J. J Food Sci 2009, 74, M46.
14. Yang, H.; Xiao, Y.; Liu, K.; Feng, Q. J Am Ceram Soc 2008, 91, 1591.
15. Fa, W.; Yang, C.; Gong, C.; Peng, T.; Zan, L. J Appl Polym Sci 2010, 118, 378.
16. Stark, N. M.; Matuana, L. M. Polym Degrad Stab 2004, 86, 1.
17. Standard Test Method for Measuring the Minimum Oxygen Concentration to support Candle-Like Combustion of Plastics (Oxygen Index), ASTM D2863; ASTM International, West Conshohocken, PA, 1997.
18. Mina, F.; Seema, S.; Matin, R.; Rahaman, J.; Sarker, R. B.; Gafur, A; Bhuiyan, A. H. Polym Degrad Stab 2009, 94, 183.
19. Han, G.; Lei, Y.; Wu, Q.; Kojima, Y. J Polym Environ 2008, 16, 123.
20. Liu, J; Chen, G.; Yang, J. Polymer 2008, 49, 3923.
21. De Rosa, C.; Corradini, P. Macromolecules 1993, 26, 5711.
22. Leung, Y. H.; Djuriic, A. B.; Gao, J.; Xie, M. H.; Wei, Z. F.; Xu, S. J.; Chan, W. K. Chem Phys Lett 2004, 394, 452.
23. Chae, D. W.; Kim, B. C. J Appl Polym Sci 2006, 99, 1854.
24. Pracella, M.; Chionna, D.; Ishak, R.; Galeski, A. Polym Plast Technol Eng 2004, 43, 1711.
25. He, J; Shao, W.; Zhang, L.; Deng, C.; Li, C. J Appl Polym Sci 2009, 114, 1303.
26. Li, H.; Tripp, C. P. Langmuir 2002, 18, 9441.
27. Dhoke, S. K.; Khanna, A. S.; Sinha, T. J. M. Prog Org Coat 2009, 64, 371.
28. Das, G.; Karak, N. Prog Org Coat 2009, 66, 59.
29. Deka, B. K.; Maji, T. K. Compos Sci Technol 2010, 70, 1755.
30. Awal, A.; Ghosh, S. B.; Sain, M. J Therm Anal Calorim 2010, 99, 695.
31. Salemane, M. G.; Luyt, A. S. J Appl Polym Sci 2006, 100, 4173.
32. Sailaja, R. R. N. Compos Sci Technol 2039 2006, 66.
33. Faruk, O.; Matuana, L. M. Compos Sci Technol 2073 2008, 68.
34. Fung, K. L.; Li, R. K. Y.; Tjong, S. C. J Appl Polym Sci 2002, 85, 169.
35. Meng, Y. Z.; Tjong, S. C. Polymer 1999, 40, 2711.
36. Yemele, M. C. N.; Koubaa, A.; Cloutier, A.; Soulounganga, P.; Wolcott, M. Compos Part A: Appl Sci 2010, 41, 131.
37. Bouza, R.; Pardo, S. G.; Barral, L.; Abad, M. J Polym Compos 2009, 30, 880.
38. Laachachi, A.; Ruch, D.; Addiego, F.; Ferriol, M.; Cochez, M.; Lopez Cuesta, J. M. Polym Degrad Stab 2009, 94, 670.
49. Zhao, H.; Li, R. K. Y. Polymer 2006, 47, 3207.
40. Grigoriadou, I.; Paraskevopoulos, K. M.; Chrissafis, K.; Pavlidou, E.; Stamkopoulos, T. G.; Bikiaris, D. Polym Degrad Stab 2011, 96, 151.
41. Camino, G.; Tartagilione, G.; Frache, A.; Manferti, C.; Costa, G. Polym Degrad Stab 2005, 90, 354.